ESC European Society of Cardiology

Cardiovascular Research (2025) **00**, 1–14
https://doi.org/10.1093/cvr/cvae267

Intestinal interstitial fluid isolation provides novel insight into the human host-microbiome interface

Ellen G. Avery[1,2,3,4,5‡], Lea-Maxie Haag[6,7‡], Victoria McParland[1,2,3], Sarah M. Kedziora[1,2,3,4], Gabriel J. Zigra[6], Daniela S. Valdes[1,2,3,4], Marieluise Kirchner[8,9], Oliver Popp[9], Sabrina Geisberger[1,10], Olivia Nonn[1,2,3,4], Tine V. Karlsen[11], Gabriele N'Diaye[2,3], Alex Yarritu[1,2,3,4], Hendrik Bartolomaeus[1,2,3,4], Theda U.P. Bartolomaeus[1,2,3,4], Nurana A. Tagiyeva[1,2,3,4], Moritz I. Wimmer[1,2,3,12], Nadine Haase[1,2,3,4], Yiming D. Zhang[1,10], Andreas Wilhelm[13], Gerald Grütz[13], Olav Tenstad[11], Nicola Wilck[1,2,3,4,14], Sofia K. Forslund[1,2,3,4], Robert Klopfleisch[15], Anja A. Kühl[6,16], Raja Atreya[17], Stefan Kempa[1,10], Philipp Mertins[8,9], Britta Siegmund[6], TRR241 IBDome Consortium, Helge Wiig[11*¶], and Dominik N. Müller[1,2,3,4*¶†]

[1]Max Delbrück Center for Molecular Medicine in the Helmholtz Association, Berlin, Germany; [2]Experimental and Clinical Research Center, a Cooperation of Charité-Universitätsmedizin Berlin and Max Delbrück Center for Molecular Medicine, Berlin, Germany; [3]Charité—Universitätsmedizin Berlin, Corporate Member of Freie Universität Berlin and Humboldt-Universität zu Berlin, Berlin, Germany; [4]DZHK (German Centre for Cardiovascular Research), Partner Site Berlin, Berlin, Germany; [5]Department of Biology, Chemistry, and Pharmacy, Freie Universität Berlin, Berlin, Germany; [6]Department for Medicine (Gastroenterology, Infectious Diseases, Rheumatology) Charité—Universitätsmedizin Berlin, Corporate Member of Freie Universität Berlin, Humboldt-Universität zu Berlin and Berlin Institute of Health, Campus Benjamin Franklin, Berlin, Germany; [7]Berlin Institute of Health at Charité—Universitätsmedizin Berlin, BIH Biomedical Innovation Academy, BIH Charité Clinician Scientist Program, Charitéplatz 1, Berlin 10117, Germany; [8]Core Unit Proteomics, Berlin Institute of Health at Charite—Universitätsmedizin Berlin, Berlin, Germany; [9]Proteomics Platform, Max Delbrück Center for Molecular Medicine, Berlin, Germany; [10]Integrative Proteomics and Metabolomics Platform, Max-Delbrück-Center for Molecular Medicine in the Helmholtz Association, Berlin Institute for Medical Systems Biology (BIMSB), Berlin, Germany; [11]Department of Biomedicine, University of Bergen, Jonas Lies vei 91, Bergen N-5009, Norway; [12]Faculty of Medicine, Universität Tübingen, Tübingen, Germany; [13]CheckImmune GmbH, BerlinBioCube, Robert-Rössle Str. 10, Berlin 13125, Germany; [14]Medizinische Klinik mit Schwerpunkt Nephrologie und Internistische Intensivmedizin, Charité—Universitätsmedizin Berlin, Berlin 13353, Germany; [15]Department of Veterinary Medicine, Freie Universität Berlin, Berlin, Germany; [16]Charité-Universitätsmedizin Berlin, Corporate Member of Freie Univeristät Berlin and Humboldt Universität zu Berlin, iPATH, Berlin, Berlin, Germany; and [17]Department of Medicine 1, Friedrich-Alexander University, Erlangen, Germany

Received 26 July 2024; revised 13 October 2024; accepted 12 November 2024; online publish-ahead-of-print xx xx 0000

Time of primary review: 47 days

Aims

The gastrointestinal (GI) tract is composed of distinct sub-regions, which exhibit segment-specific differences in microbial colonization and (patho)physiological characteristics. Gut microbes can be collectively considered as an active endocrine organ. Microbes produce metabolites, which can be taken up by the host and can actively communicate with the immune cells in the gut lamina propria with consequences for cardiovascular health. Variation in bacterial load and composition along the GI tract may influence the mucosal microenvironment and thus be reflected its interstitial fluid (IF). Characterization of the segment-specific microenvironment is challenging and largely unexplored because of lack of available tools.

Methods and results

Here, we developed methods, namely tissue centrifugation and elution, to collect IF from the mucosa of different intestinal segments. These methods were first validated in rats and mice, and the tissue elution method was subsequently translated for use in humans. These new methods allowed us to quantify microbiota-derived metabolites, mucosa-derived cytokines, and proteins at their site-of-action. Quantification of short-chain fatty acids showed enrichment in the colonic IF. Metabolite and cytokine analyses revealed

* Corresponding authors: Tel: +47 906 44 029, E-mail: helge.wiig@uib.no; Tel: +49 30 450540286; fax: +49 30 450540900, E-mail: dominik.mueller@mdc-berlin.de.
‡ Co-signing first authors.
¶ Co-signing senior authors.
† Lead Contact.

differential abundances within segments, often significantly increased compared to plasma, and proteomics revealed that proteins annotated to the extracellular phase were site-specifically identifiable in IF. Lipopolysaccharide injections in rats showed significantly higher ileal IL-1β levels in IF compared to the systemic circulation, suggesting the potential of local as well as systemic effect.

Conclusion Collection of IF from defined segments and the direct measurement of mediators at the site-of-action in rodents and humans bypasses the limitations of indirect analysis of faecal samples or serum, providing direct insight into this understudied compartment.

Keywords Interstitial fluid • Intestinal microenvironment • Microbiome • Intestine • Fluid isolation • Rodents • Humans

1. Introduction

The gut microbiota consists of a complex community of bacteria that is essential for immune homeostasis and has important implications for host health.[1] It is considered as an endocrine organ, producing metabolites that interface with host physiology by triggering responses in the local intestinal microenvironment or in distant target organs.[2] Microbiomes from diseased and non-diseased individuals differ (exhibiting a *dysbiotic* as opposed to *eubiotic* state), as shown for several inflammatory conditions (e.g. colitis), hypertensive cardiovascular disease (CVD), and metabolic disorders.[3–13] Low-grade inflammation can be triggered through dysbiosis and its derived metabolites.[14]

Combining clinical and experimental studies, we identified microbial short-chain fatty acids (SCFA) and tryptophan metabolites[15–20] to be important for CVD and multiple sclerosis (MS). SCFA (acetate, propionate, and butyrate) exert beneficial effects on the host.[13,21,22] We showed that propionate decreases inflammation, blood pressure, and cardiac damage in mice, which is in part mediated by Treg.[17] Although it is well recognized that there is considerable variability in the microbes that colonize the intestinal segments, current microbiome research mainly focuses on faecal samples, thereby losing segment-specific information. The use of faeces to study the segment-specific host-microbiota interactions may therefore be considered as disadvantage, as this sample represents only the total end-product of a highly dynamic system. Thus, we aimed to develop methods to collect interstitial fluid (IF) from different segments of the intestinal mucosa of rodents and humans to gain direct insight into the site-specific microenvironment of the gut.

IF is simply defined as the fluid found in the spaces between the cells of a tissue, the tissue's structural components known as the extracellular matrix, and the capillaries.[23] The extracellular fluid space consists primarily of IF and a small percentage of plasma.[24] Isolated IF has been used to reveal tissue-specific microenvironmental signatures present in the extracellular space, which cannot be predicted by serum measurements.[25] demonstrating the importance of measuring IF content locally at the site-of-inflammation.

The gastrointestinal (GI) tract is the interface between the host and its microbiota. We assume that the intestinal IF is rich in both host-produced and microbially produced factors such as cytokines, metabolites, and proteins, although this has not yet been demonstrated. Little is currently known about the spatial composition in the intestinal mucosal interstitium, the interaction with immune cells and the consequences for health, particularly in inflammatory and cardiovascular diseases.[26] To overcome the limitations of existing approaches, we aimed to develop and validate new methods that can be applied to rodent and human biopsies, allowing direct phenotyping of the local intestinal microenvironment instead of indirect phenotyping of faecal samples.

2. Methods

Detailed description of all analytical methods and data analysis used is available in the Supplementary material online. Experiments were carried out in both Berlin, Germany at the ECRC as well as the Bergen, Norway at the University of Bergen. All animal experiments were approved by local authorities (for Berlin: C57BL/6J mice: X9009/18, SD rats: Y9004/18; for Bergen approval ID #10508 and #13922) and all procedures were in accordance with the guidelines of the European Parliament Directive 2010/63/EU on the protection of animals used for scientific purposes or the NIH Guide for the Care and Use of Laboratory Animals. For all procedures, rats were anaesthetized with isoflurane in oxygen (4% induction, 1.5% maintenance, flow rate, and 1–2 L/min). Rats were sacrificed while under isoflurane anaesthesia (5%) either by decapitation or by excision of the heart and mice were sacrificed by cervical dislocation following isoflurane anaesthesia (5%).

3. Results

3.1 Intestinal IF can be isolated from rats by tissue centrifugation

The centrifugation technique to isolate native IF was first described for skin and tumours in rats.[27] To investigate whether this method could be applied to extract IF from the gut interstitium in rats, we excised the entire gut immediately after euthanasia. Gut segments were placed on a nylon mesh and subjected to 400 *g* for 10 min (*Figure 1A*). Following centrifugation, the volume was determined, and the isolated fluid was aliquoted for further analysis. The average fluid yield from the different segments ranged from 5 µL in duodenum to 25 µL in the other segments, respectively (*Figure 1B and C*).

The origin of the isolated fluid, i.e. whether it is derived solely from the extracellular space or is 'contaminated' with intracellular fluid from tissues and blood cells, can be assessed by determining the ratio of a tracer that equilibrates only in the extracellular fluid phase and does not pass intracellularly.[27] An example of such a tracer is the non-native labelled extracellular tracer ^{51}Cr-EDTA. After a 2-h *in vivo* equilibration period of ^{51}Cr-EDTA, we harvested and centrifuged the corresponding intestinal segments (*Figure 1D*) and calculated the tracer concentration ratio in IF (centrifuged) and plasma. In these experiments, skin was included as a reference. As shown in *Figure 1D*, except for the ileum, the mean of the IF/serum ratio was <1.0, indicating that there was a slight dilution of the IF with intracellular fluid. In an attempt to validate that the fluid isolated by centrifugation reflected the intestinal microenvironment, we determined, as a proof-of-concept, levels of the antimicrobial peptide regenerating islet-derived protein 3 gamma (REG3G), which is produced by Paneth cells in the ileum through interactions directed by symbiotic bacteria.[28,29] As expected, REG3G enrichment was specific for the ileum (*Figure 1E*). The enzyme aldolase B (ALDOB) is enriched in the small intestinal segments compared to the colon (*Figure 1F*). Next, we focused on interleukin (IL)-18, which is expressed by enteric neurons and controls goblet cell expression of antimicrobial proteins.[30] The frequency of goblet cells increases from the upper to the lower GI tract.[31] IL-18 was significantly increased in the colonic IF compared to the small intestinal IF (*Figure 1G*). We next aimed to validate the site-specific production of SCFA (propionate C3 and butyrate C4) as a use case for the measurement of microbial-derived metabolites. As expected, C3 and C4 concentrations measured directly in centrifuged IF were significantly higher in the colon with a higher level in the cecum compared to the small intestine and serum (*Figure 1H* and *I*). We further asked whether the cytokine IL-1β was also produced locally in the rat intestine. Duodenal IF showed significantly higher IL-1β concentrations compared to other segments of the small and large intestine as well as serum suggesting a local production (*Figure 1J*). Taken together, these data indicate that native IF isolated by the centrifugation-

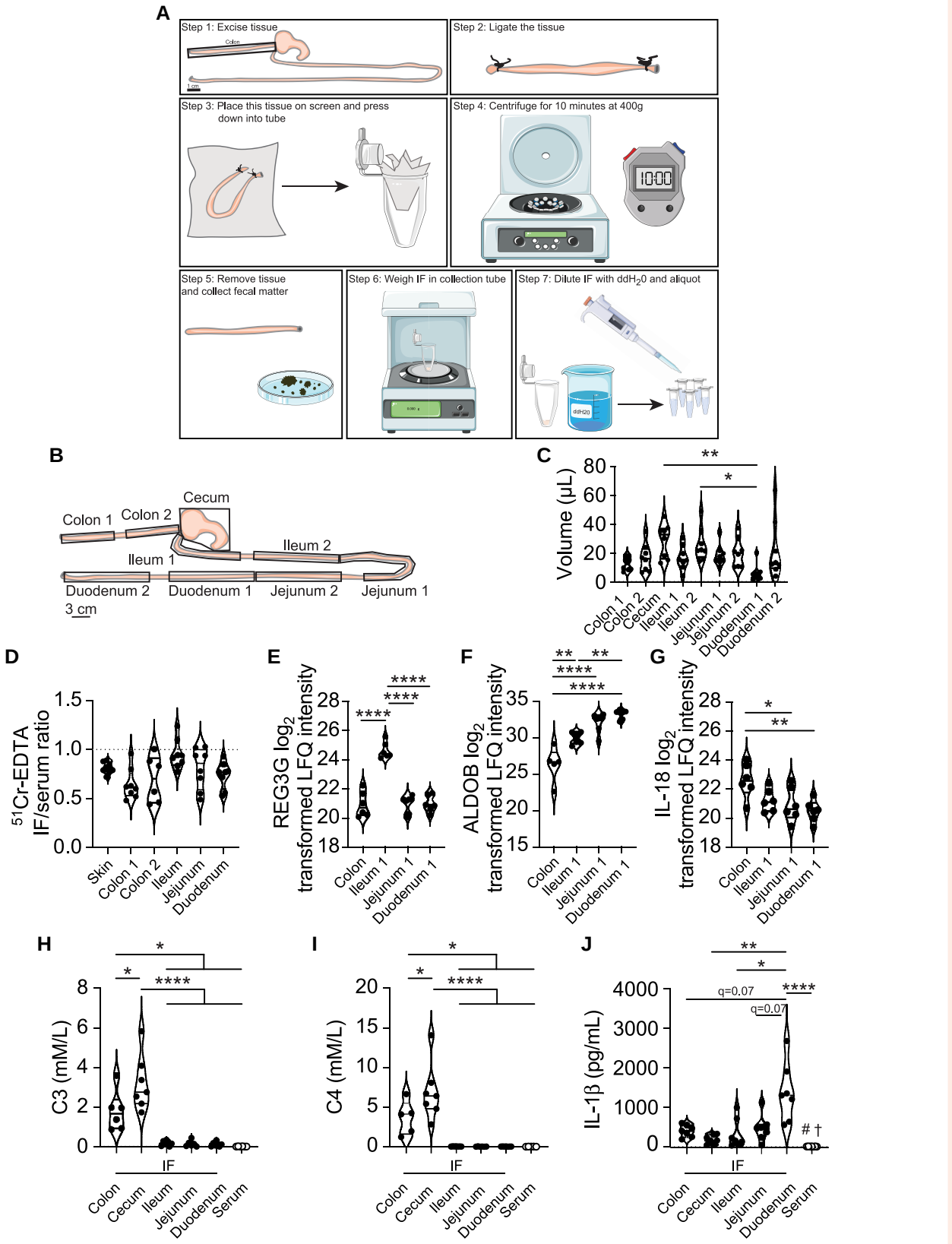

Figure 1 Centrifugation-based native extracellular fluid isolation within the GI tract of Sprague–Dawley rats. (*A*) Schematic of the centrifugation-based method for IF isolation. The GI tract was excised from just below the stomach to the colon. Seven to 10 cm pieces of GI tissue were measured, cut, and immediately ligated. The tissue was inspected for holes, and any faecal matter was squeezed out from the edges of the tissue after the ligation point. Tissue ends were trimmed if necessary. The tissue was then placed on a light screen material, folded, and in a 5 mL Eppendorf tube. Closed tubes were

(continued)

Figure 1 Continued
centrifuged for 10 min at 400 *g*. Immediately after removal of the tissue, the ligations were cut off and the faecal matter was collected. The IF from within the 5 mL Eppendorf tube was weighed, and diluent was added for aliquoting the centrifuged IF. IF was stored at −80°C for further analysis. Some images were adapted from the Servier Medical Art collection (https://smart.servier.com). (*B*) The scheme for collection of rat sample is shown. (*C*) Centrifugation volumes of IF from male and female rats ($n = 8$) as collected in (*B*). (*D*) The extracellular tracer ^{51}Cr-EDTA was used to determine how well the centrifugation method works to isolate IF from GI tissue compared to skin. The IF/serum ratio of ^{51}Cr-EDTA was determined using a gamma-counter from centrifuged IF ($n = 8$). The $\log_2$ difference of REG3G (*E*), ALDO B (*F*), and IL-18 (*G*) quantified by mass spectrometry is shown for the respective intestinal segments ($n = 6$). REG3G is selectively enhanced in the ileum, whereas IL-18 is increased in the colon. (*H–J*) Propionate (C3), butyrate (C4), and IL-1β levels of IF from different segments of the rat GI tract ($n = 5–7$ per segment). Statistical analysis for (*D*) was performed using an ordinary one-way ANOVA with Dunnett's *post hoc* test (recommended for comparison to a reference condition) applied to compare the GI tissue segment IF/serum ratio to the skin IF reference method. None of these *post hoc* comparisons were significant. Data were examined for outliers using the ROUT outlier test. Outliers were removed when appropriate. Normal distribution was tested with Shapiro–Wilk test. Data in (*C–I*) were tested by ordinary one-way ANOVA with Tukey's multiple comparison test; $*P \leq 0.05$, $**P \leq 0.01$, $****P < 0.0001$, (*J*) with Kruskal–Wallis test corrected for multiple comparisons by controlling FDR (Benjamini, Krieger, Yekutieli) $\#P < 0.002$ vs. colon and jejunum, $\dagger P < 0.05$ vs. ileum.

based method in a rat model is suitable for analytical phenotyping of microbial or intestinal-derived metabolites, cytokines, or proteins.

3.2 Isolation of intestinal IF from mice using tissue elution

Since the mouse is a preferred model in many biomedical contexts, and we therefore investigated the possibility of isolating murine IF. First, we assessed the extracellular volume (ECV) in different GI segments, as this provides information on the feasibility (see Supplementary material online, *Figure S1A*) of extracellular tracer experiments with ^{51}Cr-EDTA. The ECV of GI tissue was relatively similar to that of muscle tissue,[23] with an estimated volume of 0.1 to 0.2 mL/g wet weight, depending on the segment of interest (see Supplementary material online, *Figure S1B*). Total tissue water [the ECV and intracellular volume (ICV)] within a given tissue was also determined from the colon, cecum, ileum, jejunum, and duodenum (see Supplementary material online, *Figure S1C*). There were some very small but significant differences in the total tissue water for individual segments, although these are unlikely to be physiologically relevant. The maximum difference between any segments was 0.02 mL/g and the mean total tissue water value across all samples was 0.79 mL/g (see Supplementary material online, *Figure S1C*).

These distribution volume experiments indicated that the IF space was of a size making IF isolation by centrifugation feasible. We therefore applied the same centrifugation approach to mouse intestinal tissue. As might be expected due to the lower total tissue weight of the GI tract, IF sample volumes were smaller than in rats. Although these experiments suggested that the centrifugation method was feasible for isolation of mouse intestinal IF, the sample volumes (about 0.5 to 4 µL depending on the segment) were insufficient to overcome the limit of detection for many analyses unless pooled. We therefore developed an elution-based method to phenotype the mouse compartment. Elution-based methods have previously been used to isolate IF from various tumour tissues and are advantageous because they result in a large volume of fluid, which can be used for multiple measurements.[23] The general principle of the method is that the cleaned excised tissue is placed in an isosmotic buffer to maintain tissue integrity and osmotic pressure. Substances dissolved in the IF phase will equilibrate with the surrounding buffer by diffusion over time. The eluate is diluted relative to the original IF in the native tissue, but the dilution factor is known and can be used to calculate the tissue concentration of the analytes. Schematics of the methodological details are shown in *Figure 2A*.

Saline is a typical state-of-the-art isosmotic buffer option for elution. In the initial phases of method development, the ionic composition of IF was used as a proxy to measure the efficacy of the elution method, making saline inappropriate, and we used mannitol as the eluent. Theoretically, the ionic composition of IF should closely resemble that of plasma with low levels of potassium (K^+; 3.5–5.0 mmol/L) and levels of sodium (Na^+) ions around 140 mmol/L[23,32] and thus a ratio of IF Na^+ to serum Na^+ close to 1.0. To optimize the use of elution from GI tissues, we tested different elution time points (8 and 24 h) and analysed their effect on IF ion levels (*Figure 2B* and *C*). The longer 24 h time point resulted in higher K^+ in eluted samples ranging from 20 to 40 mmol/L (*Figure 2C*). Increased K^+ levels indicate leakage of intracellular K^+ into the eluate and/or decreased Na^+/K^+ ATPase activity, which may be a result of energy deficit of the eluted tissue and loss of tissue integrity. Thus, we used shorter elution time points for comparison (2, 4, and 8 h) and repeated the experiment with a larger number of intestinal segments. Across all segments, shorter elution times resulted in less K^+ deposited in the elution buffer (*Figure 2D* and *E*). The K^+ level within any given elution IF sample was still far higher than serum (*Figure 2E*), although this was not entirely unexpected, given the strong gradient of intracellular K^+ and high ICV relative to ECV in the GI tract. These experiments suggest that there is a significant leakage of K^+ ions originating from the intracellular space. The IF/serum Na^+ ratio was significantly different from 1.0 (*Figure 2B*), indicating that this fluid shift was accompanied by cell water.

Since ion chromatography measurements of shorter elution times suggested an improved tissue integrity, we next tested whether the substances of interest would be efficiently extracted from the intestinal IF at these lower time points. The extracellular tracer ^{51}Cr-EDTA (molecular weight = 339) mimics the size of a small molecule/metabolite and was used to assess the time likely required for a compound to equilibrate with the elution buffer (see Supplementary material online, *Figure S2*). The amount of tracer in the elution buffer was assessed relative to the total amount of tracer in each respective tissue segment. ^{51}Cr-EDTA equilibrated with the surrounding elution buffer rather quickly, with most of the tracer being eluted after 2 h (see Supplementary material online, *Figure S2*). In the small intestinal segments, there was more variation in the eluted tracer fraction. We suspect that this is due to the lower ECV in the small intestine (see Supplementary material online, *Figure S1B*), as it is known that IF is more difficult to be mobilized from spaces with a lower IF fraction.[23] Even at the longest time point studied, a small amount of the ^{51}Cr-EDTA was not recoverable, as indicated by an eluted fraction unequal to 1.0. This suggests that there may be some unspecific binding of the ^{51}Cr-EDTA within the tissue, rendering a fraction of this molecule inaccessible. Nevertheless, based on these results it is likely that small molecules such as microbiota-derived metabolites can rapidly equilibrate within the elution fluid.

3.3 IF collected using elution can be used to study tissue-specific proteomic signature

Next, we examined whether the IF from the GI tract has a protein signature that is distinct from the circulating blood as previously shown for microenvironments such as tumours[32,33] and the skin.[25] Shotgun proteomics was used to identify similarities and differences between the IF (see Supplementary material online, *Table S1*) and serum from C57BL/6 mice. Overall, significantly more unique protein IDs were found in IF compared

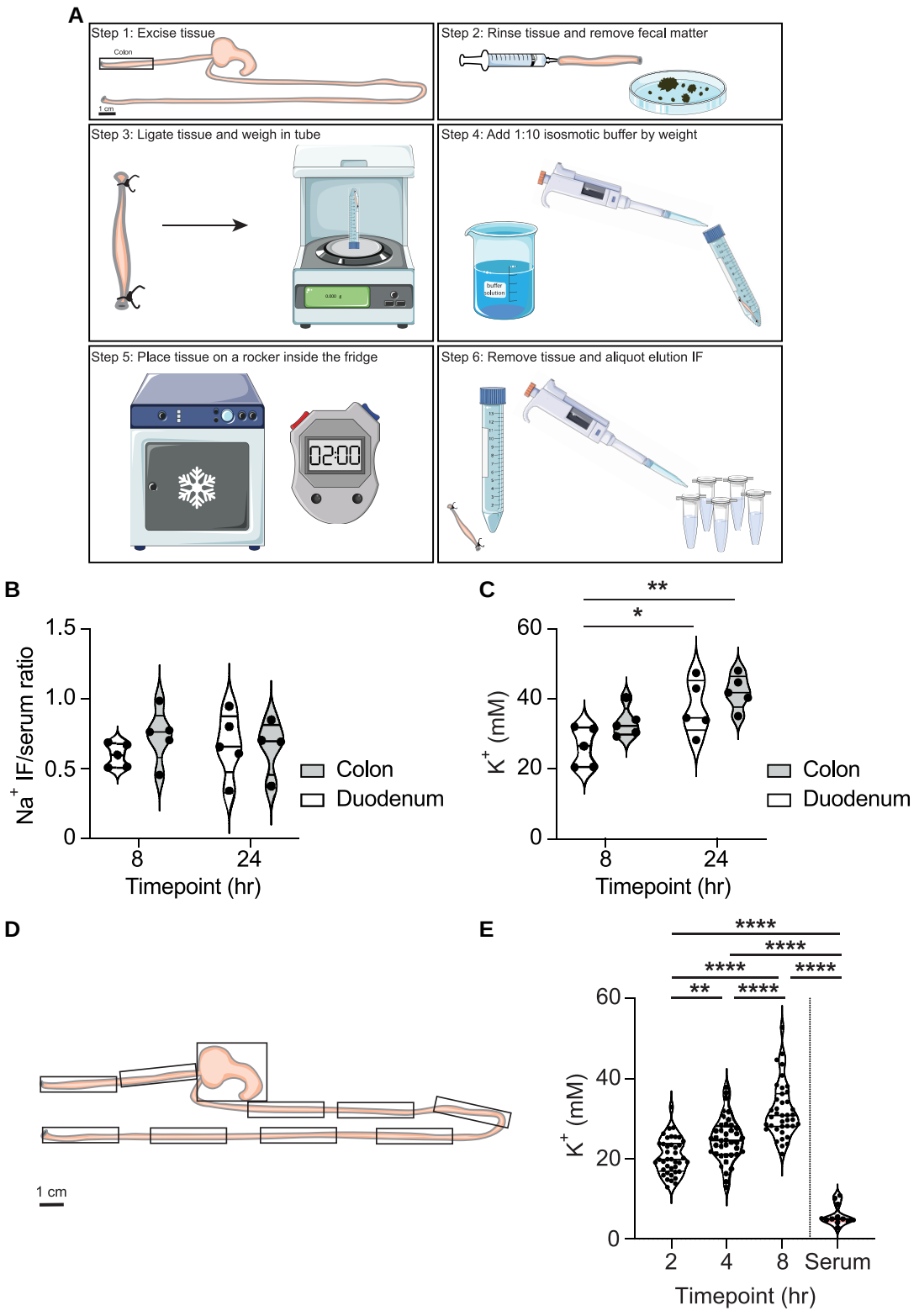

Figure 2 Schematic for the collection of IF using an elution-based method. (*A*) The respective GI tract tissue was excised and immediately washed from the luminal side using a blunt syringe with ~5 mL of isotonic buffer to ensure the removal of any luminal contents. Faecal matter was collected from the indicated segment prior to rinsing. Both ends of the tissue were ligated to ensure that if any microscopic luminal contents were still attached to the inner surface of the gut, they would not be extracted into the surrounding buffer. After ligation, the tissue was placed in a 1:10 dilution of an appropriate isosmotic buffer solution and placed on a rocker at 4°C. After the specified elution time, the tissue was removed, and the eluted fluid was aliquoted and stored at −80°C for further analysis. Some images were drawn with Servier Medical Art from Servier, licensed under a Creative Commons Attribution 3.0 Unported License (https://smart.servier.com). (*B*) Segments were taken from each region of the colon and duodenum and were either placed in mannitol for 8 or 24 h, respectively. (continued)

Figure 2 Continued
Comparison of the Na^+ IF to serum ratio (*B*) and IF K^+ (*C*) by ion chromatography from samples eluted in a mannitol-based buffer for 8 or 24 h. N = 5 for all conditions, and one outlier was excluded. (*D*) The segmentation approach from C57BL/6J mice. (*E*) K^+ was measured from IF and serum (matched by animal). Separate animals were processed for each time point, $n = 4$ for each of the 10 segments at each time point. The results from each time point were binned, and the results from each segment are shown together. Shorter time points result in significantly less K^+ (mM) in elution IF. Two-way ANOVA and *post hoc* Sidak multiple comparison test were used to test significance. *P*-values are as follows; $*P \leq 0.05$, $**P \leq 0.01$.

to serum (*Figure 3A* and *B*). Of these, 1802 proteins were statistically significantly different between elution IF and serum (*Figure 3C*). While many proteins from the serum and IF spaces overlapped (*Figure 3C*), 2581 were found to be unique to the IF space, of which 1404 were shared between the colon and duodenum segments. There was a much greater overlap in the identifiable proteins between these two IF groups than with the serum (*Figure 3C*). The normalization for these data were based on the amount of protein in the starting material rather than per volume of IF or serum. Because the protein concentration in IF is typically lower than in serum[23] and because we measured an equal amount of several peptides from each matrix in shotgun proteomics experiments, we expect that there may be a slight over-representation of some proteins in the elution IF. Nevertheless, proteins which have been documented to be highly abundant in serum, such as albumin (ALB),[23] did indeed appear to be significantly higher in serum compared to elution IF (*Figure 3B*). Notwithstanding this fact, IF may be a better way to study proteins relevant to GI health and disease, which are present or undetectable in serum due to the increased coverage of proteins from the IF space compared to the serum. Encouragingly, within the group of proteins which were robustly identifiable from the IF, there were some candidates such as galectin-3 (LGALS3; *Figure 3D*)[34] that have a known biological function in the GI tract. Antimicrobial peptides such as α-defensins (DEFA) are produced by Paneth cells. As expected, the DEFA cluster 6/9/11/15/24 was significantly enriched in mouse duodenal IF (*Figure 3E*). In line with this, ALDOB was also significantly enriched in the duodenum (*Figure 3F*) as in the native rat IF (*Figure 1F*). Next, we demonstrated that the elution method can detect SCFA (C3 and C4) in colonic IF (*Figure 3G* and *H*). Of note, colonic and cecal C3 levels were 150- and 280-fold higher, respectively compared to plasma. For C4, the respective fold change was even more pronounced (200 and 900-fold). These concentrations are based on the assumption that the substances are distributed throughout the entire fluid phase (total tissue water) of 0.79 mL/g tissue. However, if they distribute only or partially in the IF phase of 0.1–0.2 mg/g tissue, which is a reasonable assumption, their concentration will be several times higher. The same reasoning applies to eluted human samples (see below).

Next, we sought to confirm that the elution-based method recapitulated the signature observed with the centrifugation method. For these experiments, we used the SD rat model, as the larger GI tissue was suitable for direct comparisons between the two methods. Indeed, REG3G and ALDOB obtained by the elution method (*Figure 4A* and *B*; Supplementary material online, *Table S2*) showed a similar pattern in colonic IF as in the native IF of the centrifugation method (*Figure 1E* and *F*; Supplementary material online, *Table S2*), with significantly lower abundance compared to small intestinal segments of rats. Similarly, IF concentration of IL-18 was significantly higher in the colon using both the centrifugation and elution methods (*Figures 4D and 1G*; Supplementary material online, *Table S2*). Additionally, LGALS3 and ALDOB were regulated in the rat elution IF (*Figure 4B* and *C*; Supplementary material online, *Table S2*) similar to what was shown in mice (*Figure 6D* and *F*, respectively). Mass spectrometry analyses of rat IF isolated by the elution method also confirmed the pattern of SCFA (propionate C3 and butyrate C4; *Figure 4E* and *F*) observed in the native IF collected by the centrifugation method. A significant source of propionate involves conversion of dietary fibre via the succinate pathway and the methylmalonyl-CoA decarboxylase expressed in species of the Bacteroidetes. qPCR analyses show that Bacteroidetes (see Supplementary material online, *Figure S3A*) is a highly abundant phylum in the mouse colon and much less represented in the other gut sections. Furthermore, the *mmdA* enzyme (see Supplementary material online, *Figure S3B*) was only detectable by qPCR in the content of the colon and not in any other gut sections.

Given the high sensitivity of the proteomics method used, head-to-head comparison of the two methods initially revealed apparent method-specific clustering (data not shown). After independent z-scoring within the centrifugation and elution methods, a selection of inflammatory response and immune response annotations (a total of 285 proteins) from the rat Uniprot database is shown by principal component analysis (PCA; *Figure 4G*) and Pearson's correlation (*Figure 4H*). The overall proteomic signature showed a similar congruence between segments (data not shown). Segments from the small intestine overlapped to some extent, whereas the colon clustered independently from the rest of the GI tract. The correlation between segments across methods was much higher than between all segments within a given method (*Figure 4G*). Of note, the segment with the lowest correlation between the two methods was the ileum (*Figure 4H*). While the ileum correlated with the duodenum in the centrifugation method, the ileal segment correlated better with the jejunum in the elution method the ileal segment (*Figure 4H*). This may be due to slight differences in the excised segment, as small intestinal sub-regions are difficult to grossly differentiate without histologic analysis.

We proceeded to investigate the potential of the method to detect pathophysiological changes. Lipopolysaccharide (LPS) injections are commonly used to induce a local and systemic inflammatory response in rats. We hypothesized that a LPS challenge would induce a spatial cytokine response in the different segments of the gut, which would be more pronounced than in the circulation. LPS injections resulted in a significant increase in IL-1β, IL-6, and TNF-α production in the small and large intestine compared to sham injections (*Figure 5A–C*). LPS injection also significantly increased cytokines in the systemic circulation (see Supplementary material online, *Figure S4*). Notably, LPS-induced intestinal IL-1β levels were significantly higher compared to the systemic circulation (*Figure 5D*), suggesting local synthesis. In contrast, LPS administration resulted in increased production of both intestinal and non-intestinal IL-6 and TNF-α, accompanied by elevated circulating cytokine levels (*Figure 5E and F*). In contrast to the LPS sepsis model, hypertensive CVD is rather characterized by low-grade inflammation. As expected, deoxycorticosterone (DOCA)-salt treated rats had approximately one order of magnitude lower intestinal IL-1β levels compared to LPS-treated rats. While rats treated with DOCA-salt exhibited no differences in colonic (*Figure 5G*) and ileal IL-1β (*Figure 5H*) levels compared to controls, the levels in the duodenum were significantly increased (*Figure 5I*). There was no evidence of intestinal oedema in LPS-challenged and DOCA-treated animals, as evidenced by a comparable wet-to-dry ratio of intestinal segments in the control and experimental groups (data not shown). The collective findings of these experiments indicate that substances produced locally and released into the IF may enter the general circulation and influence pathological processes in other organs.

3.4 Tissue elution for IF isolation can be translated for use in humans

Having established the isolation of IF in rodents, we turned our attention to translating the procedure to human samples. Phenotyping of the human intestinal interstitium is of interest in diseases such as inflammatory bowel disease (IBD), as this is the central compartment of disease activity. To the best of our knowledge, IF phenotyping has not been done performed

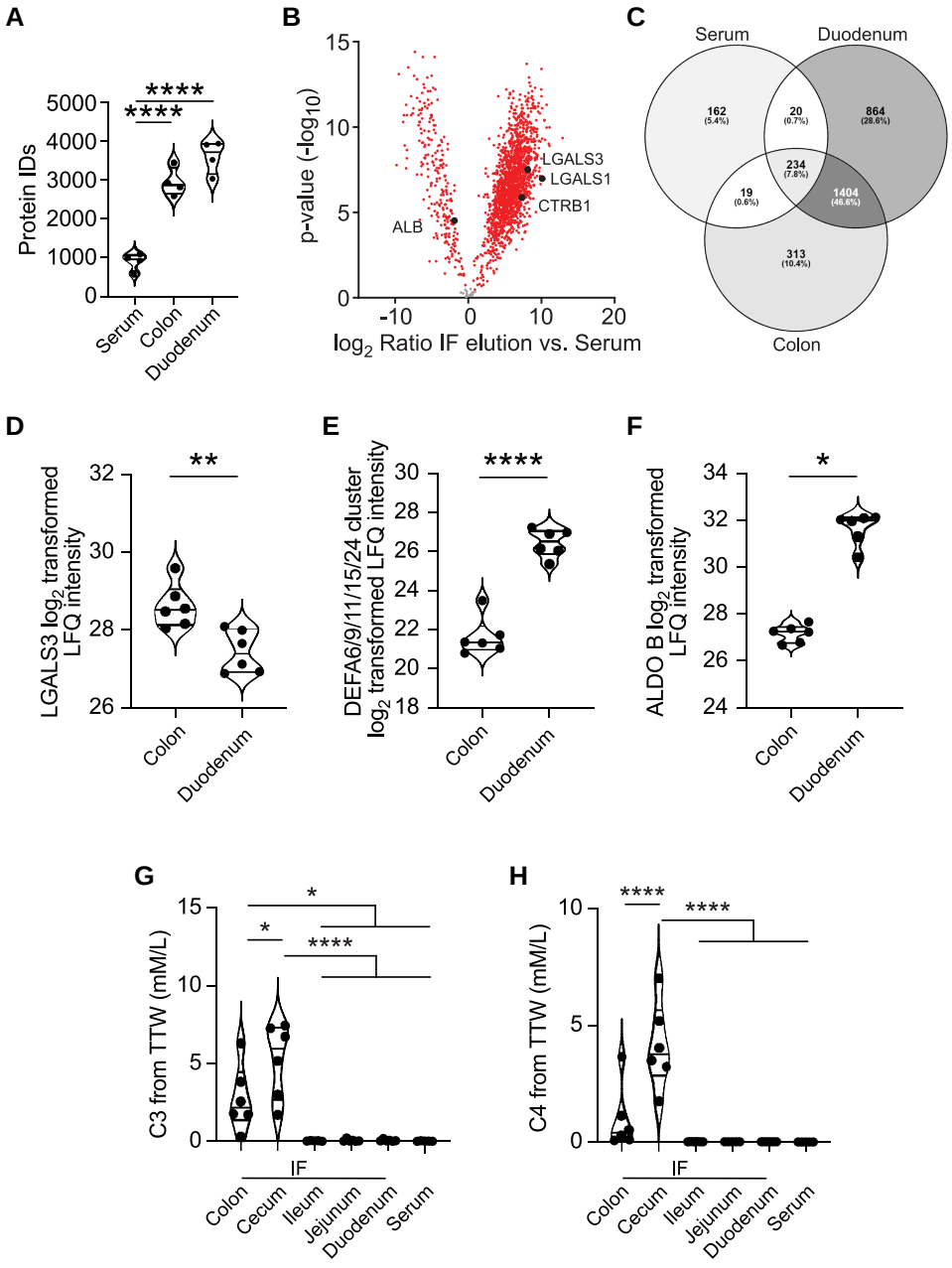

Figure 3 The serum and elution IF proteomes are unique in C57BL/6j mice. Eluate samples (colon and duodenum) from C57BL/6J mice were analysed by shotgun proteomics and compared to serum samples ($n = 4$ for each condition) for (*A–C*). Elution IF was collected after 4 h in a mannitol-based buffer solution. The Mouse Uniprot database 2019 was used for data curation. (*A*) The total number of protein IDs found in individual samples from the colon, duodenum, and serum. (*B*) Proteins which were found to be significantly different from eluate samples compared to the serum. The actual -$\log_{10}$ transformed *P*-values and the $\log_2$ difference between elution and serum for a given protein are shown as individual dots, and red dots indicate significant *P*-values after an unpaired two-tailed *t*-test with an FDR correction of 5%. The number of overlapping proteins from serum, duodenal, and colonic samples are shown in (*C*). A given protein had to have 100% valid values within at least one group to be included in the comparisons for both (*B* and *C*). The Venn diagram was generated using the Venny tool (bioinfogp.cnb.csic.es/tools/venny/index.html). A separate experiment with $n = 3$ C57BL/6J mice and two segments per anatomical segment ($n = 6$ total) was analysed using shotgun proteomics for (*D* and *E*). Elution IF was collected after 2 h in a mannitol-based solution. (*D* and *E*) Known proteins of importance in the GI tract were detectable in elution IF. The $\log_2$ transformed LFQ intensity values for individual proteins LGALS3 (*D*), the α-defensin (DEFA) cluster 6/9/11/15/24 (*E*), and ALDOB (*F*) are shown. For (*G* and *H*), samples from C57BL/6J mice ($n = 6$) were eluted for 2 h in a saline-based buffer solution for measurement of SCFA by GC-MS. (*G*) Propionate (C3) and butyrate (*H*) levels in IF from different segments of the mouse GI tract compared to plasma. Significance was tested using a paired two-tailed *t*-test for (*D* and *E*) and Wilcoxon for (*F*) and an one-way ordinary ANOVA with Tukey's multiple comparison test for (*A*, *G*, and *H*). $*P \leq 0.05$, $**P \leq 0.01$, $***P \leq 0.001$, $****P \leq 0.0001$.

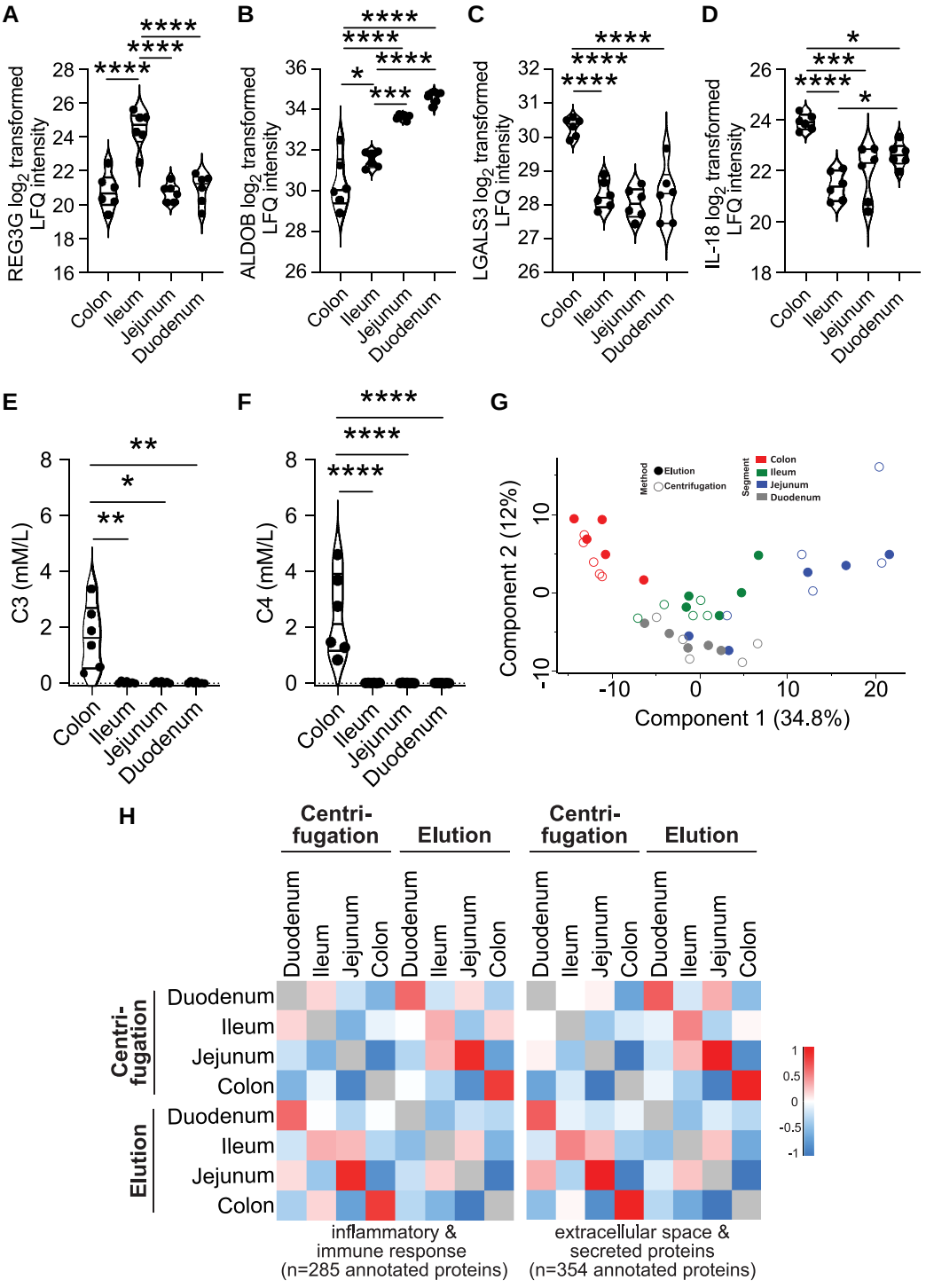

Figure 4 GI-related proteins, cytokines, and SCFA expected in IF are similarly enriched in various GI segments in both the elution and centrifugation methods. Centrifugation and elution IF were collected in tandem from SD rats ($n = 6$). Samples were eluted in saline buffer for 2 h. (*A–D*) Selected candidates (REG3G, ALDOB, LGALS3, and IL-18) were analysed by mass spectrometry in rat IF isolated by the elution method. (*E* and *F*) Propionate (C3) and butyrate (C4) levels measured by GC-MS from IF isolated by the elution method. Independent z-scoring was performed within the centrifugation and elution methods, and only proteins, which appeared with 100% valid values for at least one segment in both methods were included in the data shown in (*G* and *H*, $n = 5$). Selection of inflammatory response and immune response annotations (285 proteins) from the rat Uniprot database is shown by (*G*) PCA and (*H*) Pearson's correlation. Pearson's correlation of selected extracellular space and secreted proteins (354 proteins) from the rat Uniprot database is shown in (*H*). In (*G*), the point fill indicates the method, and the point colour indicates the segment of origin (colon, ileum, jejunum, or duodenum). In (*H*), the mean Pearson's correlation is shown for segments within and between methods. Significance for (*A–D*) was tested by ordinary one-way ANOVA with Tukey's multiple comparison test. For (*E* and *F*) Kruskal–Wallis test corrected for multiple comparison by controlling FDR (Benjamini, Krieger, Yekutieli) $*P \leq 0.05$, $**P \leq 0.01$, $***P \leq 0.001$, $****P < 0.0001$ ($n = 5$–7).

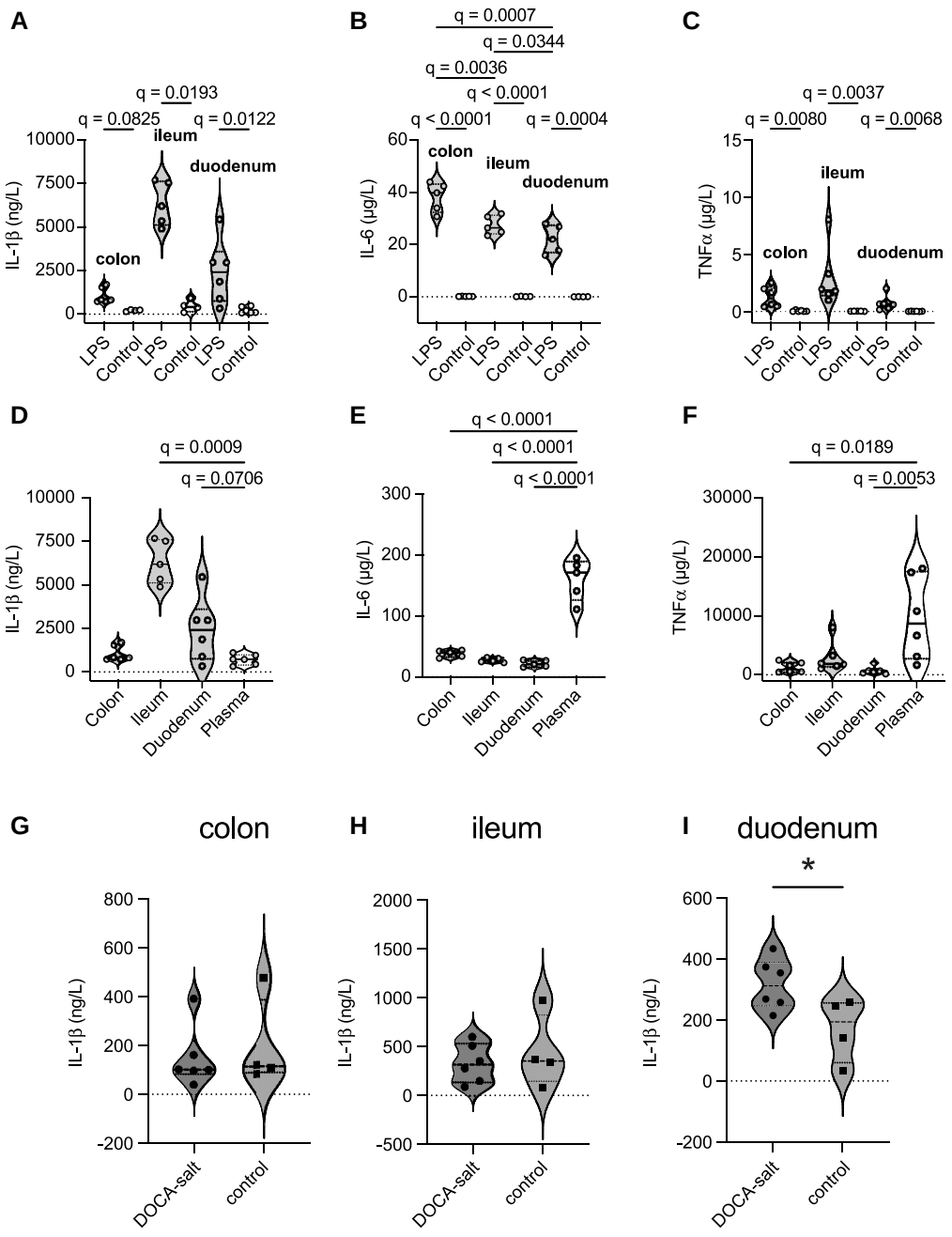

Figure 5 Cytokine levels in intestinal IF samples after LPS or DOCA-salt treatment. IL-1β (*A*), IL-6 (*B*), and TNF-α (*C*) levels of IF were significantly increased in colon, ileum, and duodenum of LPS-treated Sprague–Dawley (SD) rat ($n = 4$–6 per segment). (*D–F*) Respective IF cytokine levels were compared with plasma samples collected at the same time point. While IL-1β was increased compared to plasma, IL-6, and TNF-α were significantly higher in plasma compared to IF. (*G–I*) SD rats were implanted with a subcutaneous DOCA tablet in combination with 1% saline to drink for 6 weeks ($n = 6$) and compared with sham control SD rats ($n = 4$). IF was collected with the elution method and cytokines were measured by multiplex cytokine assays. Data were examined for outliers using the ROUT outlier test. Outliers were removed when appropriate. Data in (*A* and *C*) were tested using ordinary one-way ANOVA with Tukey's multiple comparison test with Kruskal–Wallis test and for (*B*) with Brown–Forsythe and Welch ANOVA test. (*D–F*) was corrected for multiple comparisons by controlling FDR (Benjamini, Krieger, Yekutieli). Significance for (*D* and *G*) was tested using a two-tailed Mann–Whitney *U* test and in (*E*, *F*, *H*, and *I*) using a two-tailed unpaired *t*-test.

in the context of IBD. Ideally, a method for isolation and analysis of human intestinal IF would be implementable into clinical routine and, at best, into treatment decisions. We therefore aimed to isolate IF from human intestinal mucosa biopsies obtained during colonoscopy. Of note, a colonoscopy is preceded by a routine, standardized bowel cleansing. Routine clinical human mucosal biopsies weigh an average of 9 mg, which is < 10% of the weight of rodent biopsies. Because of these very small weights, we decided to use the elution method. In this pilot study, we

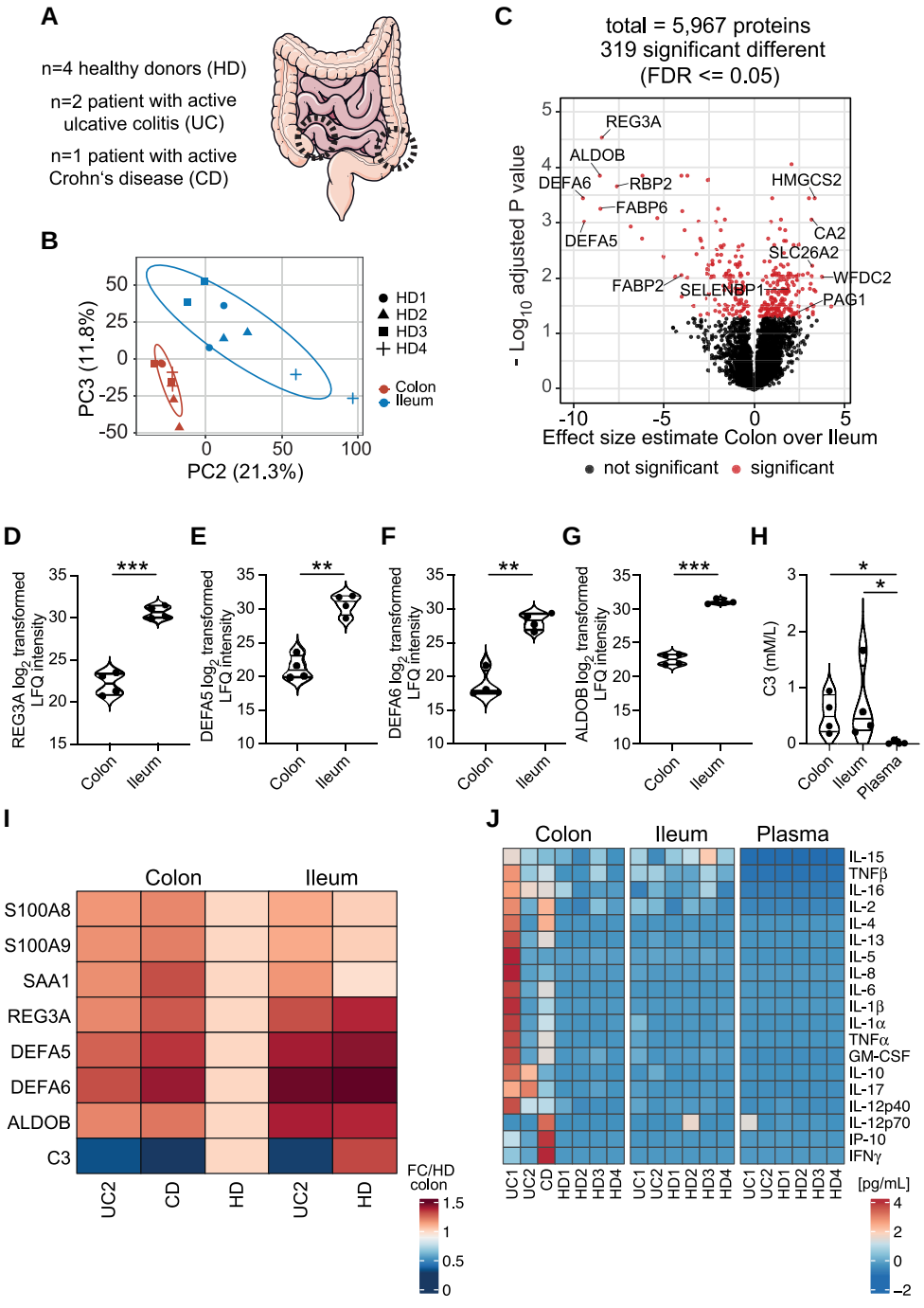

Figure 6 Distinct proteomes and cytokine signature in colon and ileum elution IF samples from healthy human donors and IBD patients. (*A*) The schematic of the human GI tract shows the location of the colon and ileum biopsy sites (dashed circles). The number of HDs ($n = 4$), patients with active UC ($n = 2$) or active CD ($n = 1$) included in the study is indicated. Part of the panel (*A*) was drawn with Servier Medical Art by Servier, licensed under a Creative Commons Attribution 3.0 Unported License. (*B–G, I*) Elution IF samples (colon and ileum) from healthy donors and diseased patients were analysed by label-free proteomics. Elution IF was collected in an isotonic sodium chloride solution for 2 h. (*B*) PCA of the IF from gut compartments of the colon and ileum of healthy donors based on 5967 proteins after data filtering. The second and third PCs represent a cumulative variance of 33.1% and separate the data sets by compartment. Two technical replicates per donor per compartment are shown, and the data were scaled and centred for PCA analysis. (*C*) Differentially regulated proteins between healthy colon and ileum samples. Each dot represents a unique protein ID plotted based on the effect size estimate and adjusted *P*-value between colon and ileum samples. Dots represent significant *P*-values tested with a paired *t*-test and a BH-FDR correction of 5%. Proteins relevant to the GI tract are highlighted. Comparison of selected candidates (REG3A, DEFA5, DEFA6, and ALDOB) in colonic and terminal ileal IF of healthy donors (*D–G*) and IBD patients (*I* and *J*) determined by performed label-free proteomics (*D–I*) or multiplex cytokine assays (*J*). (*H*) Propionate (C3) levels in colonic, ileal IF of healthy donors compared to plasma. Significance for (*D–G*) was tested using a two-tailed Welch's paired *t*-test corrected for multiple comparisons by controlling for FDR (Benjamini, Krieger, Yekutieli). For (*H*) Kruskal–Wallis test corrected for multiple comparison by controlling FDR (Benjamini, Krieger, Yekutieli) $*P \leq 0.05$, $**P \leq 0.001$, $***P \leq 0.0001$.

enrolled two patients with ulcerative colitis (UC) and one patient with Crohn's disease (CD). Furthermore, four patients undergoing surveillance colonoscopy served as healthy controls (HD). As shown in *Figure 6A*, we obtained mucosal biopsies from the highly inflamed descending colon and the terminal ileum of two patients with UC. The patient with CD presented with a severe segmental inflammation of the colon. During colonoscopy of this patient, we were able to obtain biopsies from the inflamed colon, but not from the ileum. In addition to obtaining intestinal biopsies, we drew blood to obtain paired serum samples.

First, we performed label-free proteomics and identified protein IDs ranging from 5697 to 5897 in human colon IF samples and from 5414 to 5696 in human ileum IF samples. When we compared the proteome of colonic IF samples to that of ileal IF samples from healthy donors (HDs; see Supplementary material online, *Table S3*), we found a clear separation between the two anatomical sites (*Figure 6B*). Colonic IF samples showed a high similarity between HDs, whereas ileal IF samples showed a higher variance (*Figure 5B*). A total of 5967 unique protein IDs were detected in all elution IF samples from healthy human donors (*Figure 6C*). Among these, 319 protein IDs were significantly different between the two studied intestinal sites, including several proteins known to be relevant for human GI tract health such as REG3A, DEFA5, DEFA6, and ALDOB (*Figure 6C*). As expected from the anatomical origin, antimicrobial proteins were significantly more abundant in ileal than in colonic IF (*Figure 6D–G*).

In humans, as in rodents, the terminal ileum also contains SCFA-producing microbes.[35] Therefore, it was not surprising that we detected propionate (C3) in the IF of both anatomical sites. Propionate levels in IF were more than 20-fold higher than in plasma (*Figure 6H*). Despite the cleansing procedure preceding the colonoscopy, the detected plasma levels for both propionate and butyrate (data not shown) were in a similar range compared to previous studies.[36] However, we were only able to detect propionate, but not butyrate in our eluted fluids (data not shown). Butyrate is also metabolized by colonocytes, which may be one reason for the lack of detection on addition to the effect of the bowel cleansing prior to endoscopic examination.

Shotgun proteomics (see Supplementary material online, *Table S3*) showed increased levels of S100A8 and S100A9 in IF from IBD patients, which as a heterodimer represent calprotectin (*Figure 6I*). Serum amyloid A, a robust biomarker of colorectal inflammation in UC patients, was also elevated in IF from IBD patients compared to HDs (*Figure 6I*). IBD patients had increased levels of defensin alpha 5 and 6 (DEFA5 and 6), microbicidal and cytotoxic peptides involved in the defence against bacteria and viruses, which are also prognostic markers for colorectal cancer (*Figure 6I*). Moreover, ALDOB, a protein known to enhance fructose metabolism and provide fuel during tumour cell proliferation was increased in colonic IF from IBD patients but showed no difference compared with HD in ileal IF (*Figure 6I*). Of note, despite having the same underlying active disease, each of the two UC patients had a distinct signature in their colonic IF (*Figure 6I*). The colonic IF signature for each patient was also distinct from the corresponding paired plasma sample (*Figure 6J*). This demonstrates that analysis of peripheral blood samples does not reflect the inflammatory microenvironmental signature present at the site-of-action. While UC1 had increased IL-1α and β, IL-2, IL-4, IL-5, IL-6, IL-8, and TNFα and β, GM-CSF in the colon, the second UC patient (UC2) had increased IL-17 levels (*Figure 6J*). Furthermore, our CD case showed a unique TH1-like profile which was different from the UC patients, as well as a slight induction of IL-2 and IL-4 in the colonic IF (*Figure 6J*). Anti-TNFα therapy is one treatment option in both UC and CD. Plasma TNFα levels in UC1 and UC2 were 2.8 and 2.1 pg/mL, respectively. However, in colonic IF, TNFα levels were increased 456-fold in UC1 and 40-fold in UC2 compared to plasma. While UC1 also showed 23-fold elevated ileal TNFα levels, UC2 was only 2-fold increase compared to plasma (data not shown). It is tempting to speculate whether the differences in TNFα levels within the tissue could help predict the success of anti-TNFα therapy in these patients. Taken together, spatial analysis of intestinal IF may hold promise regarding selection and prediction of therapy.

4. Discussion

The body's mucosal barriers, which separate the external environment from the internal tissues, play a critical role in maintaining host health. These selectively permeable barriers allow the entry of certain nutrients, solutes, and metabolites, which can interact and influence host (patho)-physiology. However, accessing the tissue microenvironment within the GI tract is challenging. IF representing the microenvironment within the tissue, can provide unique information about cellular processes that cannot be obtained from other fluid sources, particularly plasma. Because such fluid may not be readily available, several approaches have been applied to access the tissue microenvironment.[23] Here, we have introduced and validated two approaches to access the IF within the GI tract: tissue centrifugation and elution. We show that each of these methods can be used to understand cellular processes occurring in different segments of the intestinal mucosa and have succeeded in translating the IF collection method from rodents to humans. As use cases, we studied two experimental (cardio)vascular interventions, an LPS sepsis model and DOCA-salt, and moreover compared IBD patients during an acute flare with healthy controls to provide proof-of-principle data on the utility of our approach. Our experimental data after LPS or DOCA-salt treatment show an intestinal site-specific IL-1β production, which subsequently affect non-intestinal target organs via the circulation. Furthermore, we observed a personalized cytokine signature in colonic IF for all of our IBD patients, which we would have missed using plasma phenotyping. Taken together, these methods of IF collection have important implications for the study of the GI microenvironment and may be useful in identifying novel modulators of the microbiome-immune interface.

Sampling of IF within the tissue can be challenging regardless of the site-of-interest. When sampling is possible, prenodal lymph is likely to be the best representative of native IF, allowing assessment of the absolute concentration, which is important in determining the origin of the fluid[23] (see below). Such fluid has recently been collected from specific anatomical sites in mice and rats.[37] The sampling procedure was very laborious and resulted in ∼1 μL lymph after four to five individual cannulations per mouse. Clearly, this technique is not suitable for regular use with animal models or translatable to humans given that the fluid yield was extremely low, and the procedure is invasive and very labour intensive.

Tissue centrifugation and elution are alternative methods when prenodal lymph is not available. A major advantage with the centrifugation method is that native IF is isolated, allowing for direct quantification of mediators. Tissue elution is advantageous in that the method can be applied in situations where the amount of tissue is limited, as shown here for human intestinal mucosa biopsies. A major advantage to both techniques is that individual tissues can be sampled and used for analysis without pooling. The centrifugation technique was originally developed for IF isolation from rat tumours and skin,[27] and although it has subsequently been applied to other organs (for review see[23]) to our knowledge the method has not been evaluated for IF isolation in the gut. We have previously concluded that if the method can be validated for an organ/tissue, the centrifugation method can be considered a reference method for native IF isolation and to determine local production of substances.[23] Depending on the intestinal segment, these tracer experiments showed that intracellular fluid contributed to ∼10–40% of the isolated fluid (*Figure 1D*).

The amount of IF that can be collected from each sample is partially related to the size of the initial tissue segment. Therefore, the centrifugation technique has limitations when used with small tissue segments (mouse, human biopsies). Prospectively, however, it should be possible to obtain a larger tissue sample from resected intestinal tissue obtained during surgery, e.g. in patients suffering with IBD or intestinal malignancies. For small biopsies from colonoscopies, we have also explored the use of tissue elution for isolation of intestinal IF. This versatile technique was originally developed to isolate potential biomarker proteins from the interstitium of tumours.[38] As discussed previously,[32] the tissue preparation by sectioning described in some elution methods may result in the addition of intracellular fluid to

the eluate, thereby making it difficult to differentiate between interstitial and cellular origin of the assayed substances, a potential effect that was counteracted here by not sectioning the individual intestinal samples but leaving them otherwise intact in the buffer solution. The fact that the sample is added to a buffer during the elution procedure may pose a particular challenge when the exact concentration is required to determine whether a substance is produced locally, i.e. is an inherent part of the microenvironment, or is delivered to the tissue via the circulation.[32] However, this limitation can be overcome by back-calculation after careful consideration of dilution factors. Nevertheless, we have been able to show consistent results from elution and centrifugation experiments performed in rats and mice. Importantly, however, the proteomic database used for analysis was focused on host-specific proteins. Analysis of microbial proteins may have told a different story. Taken together, the centrifugation and elution methods have their inherent limitations but complement each other in providing access to the intestinal IF phase and microenvironment.

Differences in the anatomy, physiology, and biochemistry of the proximal and distal colon contribute to their specialized roles in digestion, absorption, and waste processing. On the one hand, the proximal colon appears to be more active in nutrient and water absorption as well as fermentation of SCFA or ethanol, whereas the distal colon is more involved in protein fermentation, the storage and final processing of faecal matter. On the other hand, patients with UC present with different local spread of the inflammation. The inflammation starts in the rectum and progresses to the descending and ascending colon, depending on the severity of the disease. Studies have shown that the interactions between immune cells and the microbiome within the GI epithelium, directly or mediated by microbial by-products, have broader implications for the host immune system in health and disease.[39] While the composition of immune cells in the gut,[31] in the draining lymph nodes,[40] and in distal organ systems[41] has been the subject of several investigations, the content of the intestinal mucosa IF, with the notable exception discussed above,[37] has been largely ignored. Interactions between humans and their intestinal inhabitants often focus on correlating phenotypic changes in the host with microbial or metabolomic signatures in faeces, which often contain a variety of undigested food residues.[42] Others have also recognized the need for alternative methods to re-evaluate the microbiome in the context of its site-specific interactions with the host. Indeed, Zmora *et al.* demonstrated that the microbiome of faecal pellets is only partially representative of the contents captured by site-specific sampling of the GI tract.[43] In a proof-of-principle study, De la Paz *et al.* demonstrated that an ingestible biosensing system can be used for *in situ* monitoring of the GI tract in a porcine model, with the goal of monitoring site-specific host-microbiome interactions in future.[44] Alternatively, the capture of IF within the GI tract may aid in our understanding of how uptake of certain molecules into the host tissue microenvironment can impact health and disease.

Translational perspective

More than 2000 years ago, Hippocrates claimed that 'all disease begins in the gut'. The ability to collect IF from tiny human intestinal biopsies and directly measure the microenvironment at the site-of-action, where microbes and mucosal immune cells reside, will overcome the limitations of indirect stool sample analysis. Our pilot proof-of-principle cytokine data pinpoint the individualized inflammatory signatures within the tissues of IBD patients. Large studies such as the *CANTOS* trial[45] in patients at risk for CVD with thousands of patients with high hsCRP have shown that anti-IL-1β treatment improves cardiovascular outcomes. Several aspects of the *CANTOS* trial inform our current work. The hsCRP-IL-1b-inflammasome axis was critical for a successful cardiovascular outcome, although large numbers of patients were needed to demonstrate benefit. Anti-inflammatory treatment was effective only in a subset of patients at risk for CVD, although identification of specific risk indicators may help to reduce treatment failures. To eventually provide patients with personalized medicine, we need to be able to identify which patients would benefit from targeted interventions. Given that our new approach can be used to identify patients with unique cytokine profiles, targeted recruitment could improve the efficacy of interventions and reduce the number needed to treat. Since the diversity of presentations and drivers of IBD flares presents a challenge, we suspect that the IF isolation from the GI tract may help us to overcome, supporting the concept of personalized medicine.

5. Limitations

Above, we have discussed the limitations of the centrifugation and elution methods *per se*. In addition, our study was intended to be a methodological proof-of-principle and feasibility study, not a clinical trial. Therefore, we analysed only three IBD patients and four healthy controls as use cases. For a more comprehensive understanding of the mucosal microenvironment, larger clinical studies are needed, which we have recently initiated (*InFlame* study; DRKS00031203). The small size of a biopsy of only about 9 mg made it impossible to obtain native fluids with the centrifugation method and forced us to use the elution method, which allows only indirect quantification. The procedure for obtaining human intestinal biopsies also has some limitations. Routinely, a bowel lavage is performed prior to the clinical colonoscopy. Thus, absolute levels of certain microbial-derived metabolites such as SCFA that are dependent on a dietary substrate, may be affected by a potential lack of continuous substrate supply due to the bowel cleansing. However, we expect that the confounding procedure would be systematic in all study participants.

Supplementary material

Supplementary material is available at *Cardiovascular Research* online.

Authors' contributions

E.G.A., L.M.H., D.N.M., and H.W. contributed to study design. E.G.A., L.M.H., S.M.K., O.N., T.V.K., A.Y., H.B., T.U.P.B., M.I.W., and O.T. contributed to data collection. G.Z., L.M.H., A.K., and B.S. collected the biopsies and were responsible for the clinical procedures. E.G.A., L.M.H., D.S.V., M.K., O.P., S.G., Y.D.Z., N.A.T., and T.V.K. contributed to data analysis. S.G. and Y.D.Z. performed SCFA measurements. N.A.T., A.W., and G.G. performed the multiplex cytokine analyses. V.Mc.P., R.K., N.H., S.M.K., P.M., B.M., N.W., S.K.F., H.W., and D.N.M. provided expert opinion and supervision. E.G.A., L.M.H., D.N.M., and H.W. contributed to manuscript preparation. TRR241 IBDome Consortium: Imke Atreya[1], Raja Atreya[1], Petra Bacher[2,3], Christoph Becker[1], Christian Bojarski[4], Nathalie Britzen-Laurent[1], Caroline Bosch-Voskens[1], Hyun-Dong Chang[5], Andreas Diefenbach[6], Claudia Günther[1], Ahmed N. Hegazy[4], Kai Hildner[1], Christoph S. N. Klose[6], Kristina Koop[1], Susanne Krug[4], Anja A. Kühl[4], Moritz Leppkes[1], Rocío López-Posadas[1], Leif S.-H. Ludwig[7], Clemens Neufert[1], Markus Neurath[1], Jay Patankar[1], Magdalena Prüß[4], Andreas Radbruch[5], Chiara Romagnani[4,5], Francesca Ronchi[6], Ashley Sanders[4,7,8], Alexander Scheffold[2,3], Jörg-Dieter Schulzke[4], Michael Schumann[4], Sebastian Schürmann[1], Britta Siegmund[4], Michael Stürzl[1], Zlatko Trajanoski[9], Antigoni Triantafyllopoulou[5,10], Maximilian Waldner[1], Carl Weidinger[4], Stefan Wirtz[1], Sebastian Zundler[1]

[1]Department of Medicine 1, Friedrich-Alexander University, Erlangen, Germany.
[2]Institute of Clinical Molecular Biology, Christian-Albrecht University of Kiel, Kiel, Germany.
[3]Institute of Immunology, Christian-Albrecht University of Kiel and UKSH Schleswig-Holstein, Kiel, Germany.
[4]Charité – Universitätsmedizin Berlin, corporate member of Freie Universität Berlin and Humboldt-Universität zu Berlin, Department of Gastroenterology, Infectious Diseases and Rheumatology, Berlin, Germany
[5]Deutsches Rheuma-Forschungszentrum, ein Institut der Leibniz-Gemeinschaft, Berlin, Germany
[6]Charité – Universitätsmedizin Berlin, corporate member of Freie Universität Berlin and Humboldt-Universität zu Berlin, Institute of Microbiology, Infectious Diseases and Immunology
[7]Berlin Institute of Health at Charité – Universitätsmedizin Berlin, Medizinische System Biologie, Charité – Universitätsmedizin Berlin
[8]Max Delbrück Center for Molecular Medicine in the Helmholtz Association, Berlin, Germany
[9]Biocenter, Institute of Bioinformatics, Medical University of Innsbruck, Innsbruck, Austria.
[10]Charité – Universitätsmedizin Berlin, corporate member of Freie Universität Berlin and Humboldt-Universität zu Berlin, Department of Rheumatology and Clinical Immunology, Berlin, Germany

Acknowledgement

We thank J. Czychi, I. Kamer, and Dr. Trude Skogstrand for their technical assistance.

Conflict of interest: The authors declare no competing interests.

Funding

B.S, A.A.K., S.K.F., P.M., N.W., and D.N.M. were all supported by the Deutsche Forschungsgemeinschaft (DFG, German Research Foundation): (DFG-SFB1449 project-ID: 321232613; B.S., S.K.F., and P.M.); (DFG-TRR 241 project-ID 375876048 as well as SFB1340 TP B06 B.S., and A.A.K.); (DFG-SFB-1365/A01 S.K.F., N.W., and D.N.M); (DFG-SFB1470/A05 S.K.F, A06 D.N.M and A10 N.W.). D.N.M. was supported by the Deutsches Zentrum für Herz-Kreislauf-Forschung, partner site Berlin (DZHK, 81Z0100110). D.N.M. and N.W. were supported by the DZGIF (DZG Innovation Fund), Topic 'Microbiome'. The German Ministry of Education and Research (BMBF) supported members of the TAhRget consortium (project-ID: 01EJ2202D D.N.M., V.McP.) and (project-ID: 01EJ2202A N.W. and H.B.). H.W. was supported by the Research Council of Norway (grant no. 262079), the Western Norway Regional Health Authority (nos F-12546 and 912168), and the Norwegian Health Association. N.W. is supported by the European Research Council under the European Union's Horizon 2020 research and innovation program grant 852796 and by the Corona Foundation in the German Stifterverband. S.G. was supported by the Bundesministerium für Bildung und Forschung (BMBF) funding Multimodal Clinical Mass Spectrometry to Target Treatment Resistance (MSTARS). L-M.H. is participant in the BIH Charité Clinician Scientist Program funded by the Charité-Universitätsmedizin Berlin and the Berlin Institute of Health at Charité (BIH).

References

1. Belkaid Y, Harrison OJ. Homeostatic immunity and the microbiota. *Immunity* 2017;**46**: 562–576.
2. Zhang LS, Davies SS. Microbial metabolism of dietary components to bioactive metabolites: opportunities for new therapeutic interventions. *Genome Med* 2016;**8**:46.
3. Forslund K, Hildebrand F, Nielsen T, Falony G, Le Chatelier E, Sunagawa S, Prifti E, Vieira-Silva S, Gudmundsdottir V, Pedersen HK, Arumugam M, Kristiansen K, Voigt AY, Vestergaard H, Hercog R, Costea PI, Kultima JR, Li J, Jørgensen T, Levenez F, Dore J, Nielsen HB, Brunak S, Raes J, Hansen T, Wang J, Ehrlich SD, Bork P, Pedersen O. Disentangling type 2 diabetes and metformin treatment signatures in the human gut microbiota. *Nature* 2015;**528**:262–266.
4. Qin J, Li Y, Cai Z, Li S, Zhu J, Zhang F, Liang S, Zhang W, Guan Y, Shen D, Peng Y, Zhang D, Jie Z, Wu W, Qin Y, Xue W, Li J, Han L, Lu D, Wu P, Dai Y, Sun X, Li Z, Tang A, Zhong S, Li X, Chen W, Xu R, Wang M, Feng Q, Gong M, Yu J, Zhang Y, Zhang M, Hansen T, Sanchez G, Raes J, Falony G, Okuda S, Almeida M, LeChatelier E, Renault P, Pons N, Batto JM, Zhang Z, Chen H, Yang R, Zheng W, Li S, Yang H, Wang J, Ehrlich SD, Nielsen R, Pedersen O, Kristiansen K, Wang J. A metagenome-wide association study of gut microbiota in type 2 diabetes. *Nature* 2012;**490**:55–60.
5. Koeth RA, Wang Z, Levison BS, Buffa JA, Org E, Sheehy BT, Britt EB, Fu X, Wu Y, Li L, Smith JD, DiDonato JA, Chen J, Li H, Wu GD, Lewis JD, Warrier M, Brown JM, Krauss RM, Tang WH, Bushman FD, Lusis AJ, Hazen SL. Intestinal microbiota metabolism of l-carnitine, a nutrient in red meat, promotes atherosclerosis. *Nat Med* 2013;**19**:576–585.
6. Tang WH, Wang Z, Fan Y, Levison B, Hazen JE, Donahue LM, Wu Y, Hazen SL. Prognostic value of elevated levels of intestinal microbe-generated metabolite trimethylamine-N-oxide in patients with heart failure: refining the gut hypothesis. *J Am Coll Cardiol* 2014;**64**: 1908–1914.
7. Tang WH, Wang Z, Levison BS, Koeth RA, Britt EB, Fu X, Wu Y, Hazen SL. Intestinal microbial metabolism of phosphatidylcholine and cardiovascular risk. *N Engl J Med* 2013;**368**: 1575–1584.
8. Schupack DA, Mars RAT, Voelker DH, Abeykoon JP, Kashyap PC. The promise of the gut microbiome as part of individualized treatment strategies. *Nat Rev Gastroenterol Hepatol* 2022;**19**:7–25.
9. Fromentin S, Forslund SK, Chechi K, Aron-Wisnewsky J, Chakaroun R, Nielsen T, Tremaroli V, Ji B, Prifti E, Myridakis A, Chilloux J, Andrikopoulos P, Fan Y, Olanipekun MT, Alves R, Adiouch S, Bar N, Talmor-Barkan Y, Belda E, Caesar R, Coelho LP, Falony G, Fellahi S, Galan P, Galleron N, Helft G, Hoyles L, Isnard R, Le Chatelier E, Julienne H, Olsson L, Pedersen HK, Pons N, Quinquis B, Rouault C, Roume H, Salem JE, Schmidt TSB, Vieira-Silva S, Li P, Zimmermann-Kogadeeva M, Lewinter C, Søndertoft NB, Hansen TH, Gauguier D, Gøtze JP, Køber L, Kornowski R, Vestergaard H, Hansen T, Zucker JD, Hercberg S, Letunic I, Bäckhed F, Oppert JM, Nielsen J, Raes J, Bork P, Stumvoll M, Segal E, Clément K, Dumas ME, Ehrlich SD, Pedersen O. Microbiome and metabolome features of the cardiometabolic disease spectrum. *Nat Med* 2022;**28**:303–314.
10. Li J, Zhao F, Wang Y, Chen J, Tao J, Tian G, Wu S, Liu W, Cui Q, Geng B, Zhang W, Weldon R, Auguste K, Yang L, Liu X, Chen L, Yang X, Zhu B, Cai J. Gut microbiota dysbiosis contributes to the development of hypertension. *Microbiome* 2017;**5**:14.
11. Robles-Vera I, Toral M, Duarte J. Microbiota and hypertension: role of the sympathetic nervous system and the immune system. *Am J Hypertens* 2020;**33**:890–901.
12. Verhaar BJH, Collard D, Prodan A, Levels JHM, Zwinderman AH, Bäckhed F, Vogt L, Peters MJL, Muller M, Nieuwdorp M, van den Born BH. Associations between gut microbiota, faecal short-chain fatty acids, and blood pressure across ethnic groups: the HELIUS study. *Eur Heart J* 2020;**41**:4259–4267.
13. Avery EG, Bartolomaeus H, Maifeld A, Marko L, Wiig H, Wilck N, Rosshart SP, Forslund SK, Müller DN. The gut microbiome in hypertension: recent advances and future perspectives. *Circ Res* 2021;**128**:934–950.
14. Warmbrunn MV, Herrema H, Aron-Wisnewsky J, Soeters MR, Van Raalte DH, Nieuwdorp M. Gut microbiota: a promising target against cardiometabolic diseases. *Expert Rev Endocrinol Metab* 2020;**15**:13–27.
15. Wilck N, Matus MG, Kearney SM, Olesen SW, Forslund K, Bartolomaeus H, Haase S, Mähler A, Balogh A, Markó L, Vvedenskaya O, Kleiner FH, Tsvetkov D, Klug L, Costea PI, Sunagawa S, Maier L, Rakova N, Schatz V, Neubert P, Frätzer C, Krannich A, Gollasch M, Grohme DA, Côrte-Real BF, Gerlach RG, Basic M, Typas A, Wu C, Titze JM, Jantsch J, Boschmann M, Dechend R, Kleinewietfeld M, Kempa S, Bork P, Linker RA, Alm EJ, Müller DN. Salt-responsive gut commensal modulates TH17 axis and disease. *Nature* 2017;**551**: 585–589.
16. Bartolomaeus H, Avery EG, Bartolomaeus TUP, Kozhakhmetov S, Zhumadilov Z, Müller DN, Wilck N, Kushugulova A, Forslund SK. Blood pressure changes correlate with short-chain fatty acids production shifts under a synbiotic intervention. *Cardiovasc Res* 2020; **116**:1252–1253.
17. Bartolomaeus H, Balogh A, Yakoub M, Homann S, Markó L, Höges S, Tsvetkov D, Krannich A, Wundersitz S, Avery EG, Haase N, Kräker K, Hering L, Maase M, Kusche-Vihrog K, Grandoch M, Fielitz J, Kempa S, Gollasch M, Zhumadilov Z, Kozhakhmetov S, Kushugulova A, Eckardt KU, Dechend R, Rump LC, Forslund SK, Müller DN, Stegbauer J, Wilck N. Short-Chain fatty acid propionate protects from hypertensive cardiovascular damage. *Circulation* 2019;**139**:1407–1421.
18. Duscha A, Gisevius B, Hirschberg S, Yissachar N, Stangl GI, Dawin E, Bader V, Haase S, Kaisler J, David C, Schneider R, Troisi R, Zent D, Hegelmaier T, Dokalis N, Gerstein S, Del Mare-Roumani S, Amidror S, Staszewski O, Poschmann G, Stühler K, Hirche F, Balogh A, Kempa S, Träger P, Zaiss MM, Holm JB, Massa MG, Nielsen HB, Faissner A, Lukas C, Gatermann SG, Scholz M, Przuntek H, Prinz M, Forslund SK, Winklhofer KF, Müller DN, Linker RA, Gold R, Haghikia A. Propionic acid shapes the multiple sclerosis disease course by an immunomodulatory mechanism. *Cell* 2020;**180**:1067–1080.e16.
19. Haghikia A, Jörg S, Duscha A, Berg J, Manzel A, Waschbisch A, Hammer A, Lee DH, May C, Wilck N, Balogh A, Ostermann AI, Schebb NH, Akkad DA, Grohme DA, Kleinewietfeld M, Kempa S, Thöne J, Demir S, Müller DN, Gold R, Linker RA. Dietary fatty acids directly impact central nervous system autoimmunity via the small intestine. *Immunity* 2015;**43**:817–829.
20. Maifeld A, Bartolomaeus H, Löber U, Avery EG, Steckhan N, Markó L, Wilck N, Hamad I, Šušnjar U, Mähler A, Hohmann C, Chen CY, Cramer H, Dobos G, Lesker TR, Strowig T, Dechend R, Bzdok D, Kleinewietfeld M, Michalsen A, Müller DN, Forslund SK. Fasting alters

the gut microbiome reducing blood pressure and body weight in metabolic syndrome patients. *Nat Commun* 2021;**12**:1970.
21. Bartolomaeus H, Markó L, Wilck N, Luft FC, Forslund SK, Muller DN. Precarious symbiosis between host and microbiome in cardiovascular health. *Hypertension* 2019;**73**:926–935.
22. Koh A, De Vadder F, Kovatcheva-Datchary P, Backhed F. From dietary fiber to host physiology: short-chain fatty acids as key bacterial metabolites. *Cell* 2016;**165**:1332–1345.
23. Wiig H, Swartz MA. Interstitial fluid and lymph formation and transport: physiological regulation and roles in inflammation and cancer. *Physiol Rev* 2012;**92**:1005–1060.
24. Bhave G, Neilson EG. Body fluid dynamics: back to the future. *J Am Soc Nephrol* 2011;**22**:2166–2181.
25. Nedrebo T, Reed RK, Jonsson R, Berg A, Wiig H. Differential cytokine response in interstitial fluid in skin and serum during experimental inflammation in rats. *J Physiol* 2004;**556**:193–202.
26. Dinakis E, O'Donnell JA, Marques FZ. The gut-immune axis during hypertension and cardiovascular diseases. *Acta Physiol (Oxf)* 2024;**240**:e14193.
27. Wiig H, Aukland K, Tenstad O. Isolation of interstitial fluid from rat mammary tumors by a centrifugation method. *Am J Physiol Heart Circ Physiol* 2003;**284**:H416–H424.
28. Vaishnava S, Behrendt CL, Ismail AS, Eckmann L, Hooper LV. Paneth cells directly sense gut commensals and maintain homeostasis at the intestinal host-microbial interface. *Proc Natl Acad Sci U S A* 2008;**105**:20858–20863.
29. Cash HL, Whitham CV, Behrendt CL, Hooper LV. Symbiotic bacteria direct expression of an intestinal bactericidal lectin. *Science* 2006;**313**:1126–1130.
30. Jarret A, Jackson R, Duizer C, Healy ME, Zhao J, Rone JM, Bielecki P, Sefik E, Roulis M, Rice T, Sivanathan KN, Zhou T, Solis AG, Honcharova-Biletska H, Vélez K, Hartner S, Low JS, Qu R, de Zoete MR, Palm NW, Ring AM, Weber A, Moor AE, Kluger Y, Nowarski R, Flavell RA. Enteric nervous system-derived IL-18 orchestrates mucosal barrier immunity. *Cell* 2020;**180**:813–814.
31. Mowat AM, Agace WW. Regional specialization within the intestinal immune system. *Nat Rev Immunol* 2014;**14**:667–685.
32. Haslene-Hox H, Tenstad O, Wiig H. Interstitial fluid-a reflection of the tumor cell microenvironment and secretome. *Biochim Biophys Acta* 2013;**1834**:2336–2346.
33. Halvorsen AR, Helland Å, Gromov P, Wielenga VT, Talman MM, Brunner N, Sandhu V, Børresen-Dale AL, Gromova I, Haakensen VD. Profiling of microRNAs in tumor interstitial fluid of breast tumors—a novel resource to identify biomarkers for prognostic classification and detection of cancer. *Mol Oncol* 2017;**11**:220–234.
34. Demetter P, Nagy N, Martin B, Mathieu A, Dumont P, Decaestecker C, Salmon I. The galectin family and digestive disease. *J Pathol* 2008;**215**:1–12.
35. Cummings JH, Pomare EW, Branch WJ, Naylor CP, Macfarlane GT. Short chain fatty acids in human large intestine, portal, hepatic and venous blood. *Gut* 1987;**28**:1221–1227.
36. Sowah SA, Hirche F, Milanese A, Johnson TS, Grafetstätter M, Schübel R, Kirsten R, Ulrich CM, Kaaks R, Zeller G, Kühn T, Stangl GI. Changes in plasma short-chain fatty acid levels after dietary weight loss among overweight and obese adults over 50 weeks. *Nutrients* 2020;**12**:452.
37. Zawieja DC, Thangaswamy S, Wang W, Furtado R, Clement CC, Papadopoulos Z, Vigano M, Bridenbaugh EA, Zolla L, Gashev AA, Kipnis J, Lauvau G, Santambrogio L. Lymphatic cannulation for lymph sampling and molecular delivery. *J Immunol* 2019;**203**:2339–2350.
38. Celis JE, Gromov P, Cabezón T, Moreira JM, Ambartsumian N, Sandelin K, Rank F, Gromova I. Proteomic characterization of the interstitial fluid perfusing the breast tumor microenvironment: a novel resource for biomarker and therapeutic target discovery. *Mol Cell Proteomics* 2004;**3**:327–344.
39. Zheng D, Liwinski T, Elinav E. Interaction between microbiota and immunity in health and disease. *Cell Res* 2020;**30**:492–506.
40. Esterházy D, Canesso MCC, Mesin L, Muller PA, de Castro TBR, Lockhart A, ElJalby M, Faria AMC, Mucida D. Compartmentalized gut lymph node drainage dictates adaptive immune responses. *Nature* 2019;**569**:126–130.
41. Madhur MS, Elijovich F, Alexander MR, Pitzer A, Ishimwe J, Van Beusecum JP, Patrick DM, Smart CD, Kleyman TR, Kingery J, Peck RN, Laffer CL, Kirabo A. Hypertension: do inflammation and immunity hold the key to solving this epidemic? *Circ Res* 2021;**128**:908–933.
42. Karu N, Deng L, Slae M, Guo AC, Sajed T, Huynh H, Wine E, Wishart DS. A review on human fecal metabolomics: methods, applications and the human fecal metabolome database. *Anal Chim Acta* 2018;**1030**:1–24.
43. Zmora N, Zilberman-Schapira G, Suez J, Mor U, Dori-Bachash M, Bashiardes S, Kotler E, Zur M, Regev-Lehavi D, Brik RB, Federici S, Cohen Y, Linevsky R, Rothschild D, Moor AE, Ben-Moshe S, Harmelin A, Itzkovitz S, Maharshak N, Shibolet O, Shapiro H, Pevsner-Fischer M, Sharon I, Halpern Z, Segal E, Elinav E. Personalized gut mucosal colonization resistance to empiric probiotics is associated with unique host and microbiome features. *Cell* 2018;**174**:1388–1405.e1321.
44. De la Paz E, Maganti NH, Trifonov A, Jeerapan I, Mahato K, Yin L, Sonsa-Ard T, Ma N, Jung W, Burns R, Zarrinpar A, Wang J, Mercier PP. A self-powered ingestible wireless biosensing system for real-time in situ monitoring of gastrointestinal tract metabolites. *Nat Commun* 2022;**13**:7405.
45. Ridker PM, Everett BM, Thuren T, MacFadyen JG, Chang WH, Ballantyne C, Fonseca F, Nicolau J, Koenig W, Anker SD, Kastelein JJP, Cornel JH, Pais P, Pella D, Genest J, Cifkova R, Lorenzatti A, Forster T, Kobalava Z, Vida-Simiti L, Flather M, Shimokawa H, Ogawa H, Dellborg M, Rossi PRF, Troquay RPT, Libby P, Glynn RJ; CANTOS Trial Group. Antiinflammatory therapy with canakinumab for atherosclerotic disease. *N Engl J Med* 2017;**377**:1119–1131.